Available online at www.sciencedirect.com

ScienceDirect

Materials Today: Proceedings 18 (2019) 1875–1881

materialstoday: PROCEEDINGS

www.materialstoday.com/proceedings

ICSMD-2017

The structural and optical properties of ZnS films optained by spraying solutions at different molarities

T. Hurma*

Department of Physics, Anadolu University, TR-26470, Eskisehir, Turkey

Abstract

ZnS films were produced by using aqueous solutions in three different concentrations. ZnS films were formed at 300±5°C on glass substrates by using ultrasonic spray pyrolysis (USP) method. The effects of sprayed aqueous solution on structural and optical characteristics of these films were analyzed. X-ray diffraction (XRD) results showed that change in solution concentration had an effect on crystallization levels and preferential orientation of the films. Crystallization sizes of the films were around 5.25-6.28 nm. The Zn-S, C-O, and C-H vibration mode peaks of films observed in Fourier transform infrared (FT-IR) spectra were symmetrical and almost at same intensity. Raman spectra taken at 100-1500 cm^{-1} range changed by increasing concentration. It was observed that ZnS films held well on the surface through the Scanning electron microscope (SEM) analyses. As molarity increased, transmittance edge shifted towards smaller wavelengths. At 350 nm wavelength, maximum transmittance value increased up to 85%. In the visible section, reflectance values of the films got very close values to each other.

Selection and/or Peer-review under responsibility of INTERNATIONAL CONGRESS ON SEMICONDUCTOR MATERIALS AND DEVICES.

Keywords: ZnS film; XRD; FTIR; Raman; Optical properties

* Corresponding author. Tel.: +90222 3350580; Fax: +90222 3204910.
E-mail address: tulayhurma@gmail.com

Selection and/or Peer-review under responsibility of INTERNATIONAL CONGRESS ON SEMICONDUCTOR MATERIALS AND DEVICES.

1. Introduction

Semiconducting thin films are either from metal and nonmetal group and they are several nanometer and micron thick films formed on materials with a fusion heat around 2000 ^{o}C. Most of the materials with semiconducting characteristics must be gathered as a thin film on a layer for using in technological applications. Thin film materials have the bulk physical properties of materials although they gain new properties in nanometer size. Intensive studies on thin films, which have begun since 1950s, have nowadays provided a wide range of use in electricity and electronics. If, we list the most important technologies which made it possible for us using current electronic devices, we can definitely say that semiconductor technology will be on the top of this list. Semiconductors as the core of all microprocessors are in transistors, flat-screen televisions and all computer-based device technologies. In addition to this, thin film technology presents us the thin film solar cells in the frame of clean and renewable power pursuit. Thin film technology is not only used in producing traditional solar cells, but also the solar cells completely consisting of thin films provides high efficiency and production facility. II-IV group compound semiconducting thin films attracted a great deal of attention due to their applications in thin film solar cells, optic coatings, optoelectronic devices and light-emitting diodes [1]. Especially, nano semiconducting materials with II-IV wide bandwidth attract more attention due to adjustable physical and chemical characteristics and various application fields [2-5]. Recently, ZnS thin films have been successfully used as glazing material for replacing CdS used in solar cells [6-9]. ZnS is more environment-friendly than CdS and it increases generated current by ensuring blue zone of the spectrum reaches to the joint due to its wide energy band gap as 3.7 eV compared to CdS films with 2.42 eV energy band gap [6,10,11]. The large band gap of the semiconductor compounds can suppress electron excitation process but at the same time excited electrons may have larger escape depth due to reduced electron scattering. Especially, these materials have a lower surface barrier potential compared to metals [12]. It is important for technological applications to determine linear optical characteristics of thin films such as thickness, refraction index, transmittance, reflectance and optical conductivity. The most important problem for researching various characteristics of thin films and using them in particular applications is to produce the thin film of a material under controlled conditions. There are several physical and chemical methods for producing thin films. Some of them can be listed as thermal evaporation [13], chemical vapor deposition [14], spray pyrolysis [15] and chemical bath deposition [16]. Each method has its specific advantages and disadvantages. USP method is one of the easiest and cheapest methods for producing thin films. Quality, bottom temperature, spray rate and solution concentration of a film produced by the USP method vary by empirical parameters. According to literature researches, crystallization levels of ZnS films are generally low [7,10,17-19]. In this study, solution concentrations were changed by keeping other parameters fixed for producing ZnS films with high crystallization levels by using USP method and structural and optical characteristics of produced films were analyzed. It is aimed to improve some material characteristics of films such as surface roughness, particle size, morphology and optical characteristics.

2. Experimental details

ZnS films were produced on glass substrates by using USP method. USP method is a very cheap and simple method which provides very good results. Also, it can be easily applied on large surfaces. In this method known as spraying, film formation process begins after fired ions perform momentum transfer by interacting target atoms and sprayed kinds are concentrated on a base for establishing a thin film formation. While, producing films by USP technique, a small change to be applied on used parameters might significantly change the thickness, forbidden energy ranges, electrical and optical properties of these films. In this study, 0.05M, 0.10M and 0.15 M $ZnCl_2$ and NH_2CSNH_2 solutions were prepared for obtaining ZnS films. 75 ml 0.05 M $ZnCl_2$ and 75 ml 0.05 M NH_2CSNH_2 solutions were mixed and the total solution to be sprayed for ZnS (0.05 M) film was prepared. Total solutions to be sprayed for ZnS (0.10 M) and ZnS (0.15 M) films were prepared in the same way. Other empirical parameters were kept fixed in the same values for all three films. Spraying rate was set 5cc/min, spraying continued for 30 minutes, base was heated up to 300±5°C, distance between the base and atomizer was set as 35 cm and 1 bar air was used as the carrier gas. Crystal structures and phases of the produced films were determined by XRD measurements. XRD measurements were done by using CuKα beam with λ=1,541 Å wavelength with BRUKER D8 Advance X-ray diffractometer. FTIR measurement has been conducted by means of ATR (4 cm^{-1} resolution) and using Perkin

Elmer 2000 FT-IR spectrometer. Raman measurements were done through Bruker Senterra Dispersive Raman system by using (He_Ne laser) x-rays at 632.8 nm wavelength at 100-1500 cm^{-1} range. The forbidden energy ranges, refraction indexes, extinction coefficients and optical conductivities of films were calculated by using transmittance and reflectance spectra taken at 200-900 nm wavelength by means of a Shimadzu 2450 UV model spectrophotometer. Surface morphology of the films was studied using scanning electron microscopy (SEM) and obtained images.

3. Result and Discussion

3.1 X-ray diffraction analysis and SEM images

When, x-rays are on a lattice plane inside the crystal, every electron existing on the plane absorbs X-rays and begins vibrating and a spherical wave begins spreading from each electron. While, X-rays penetrate through millions of lattice planes until completely absorbed and spreading waves establish supporting interferences towards specific directions where geometric conditions are available and establish damped interferences towards all other directions where conditions are unavailable. The intensity increase caused by this supporting interference gives the characteristic peaks of the structure and these peaks inform us on crystalline structure of materials. The crystalline structure and tendencies of ZnS films obtained in this study were studied by using XRD method.

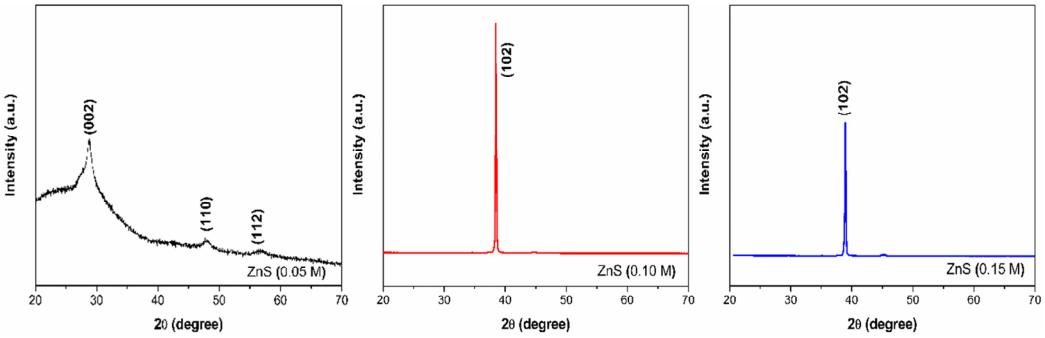

Fig. 1. XRD spectra of the ZnS nanostructured films.

All diffraction peaks shown in Fig. 1 can be indexed to ZnS hexagonal wurtzite structure (JCPDS: 775-1534) [20,21]. Diffraction peaks belong to (102) (002), (110), and (112), planes are shown in XRD spectra for the films. It was determined from the results of XRD analyses that molarities of solutions prepared for obtaining the films have significant impact on crystallization levels of the films. Crystallization level of ZnS (0.05 M) film is quite lower than other films. The highest crystallization level belongs to ZnS (0.10 M) film. While, the preferential orientation of ZnS (0.05 M) film had been towards (002) direction, it changed as (102) by increasing molarity. The crystallite size of obtained films is in nanometers. From XRD patterns, the crystallite sizes were calculated by means of Scherrer formula and ZnS for 0,05M, 0,10M and 0,15 M films was found respectively as 5.60 nm, 6,28 nm, and 5,25 nm.

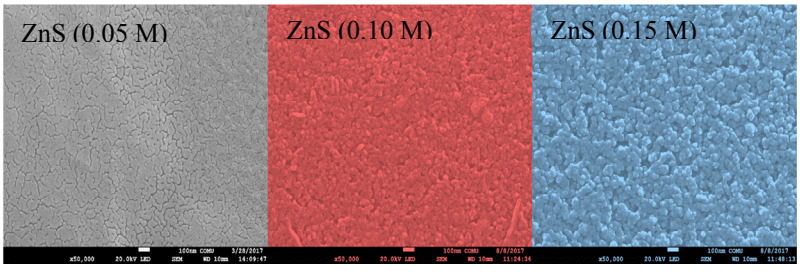

Fig. 2. SEM images of the ZnS nanostructured films.

SEM analysis is a microscopic method for obtaining image of a structure based on electrons scattered by sending electrons under high vacuum atmosphere from an electron atomizer on the structure. SEM surface images of the films were obtained by 50.000x magnification and these images are given in Fig. 2. The crystallite sizes calculated from the XRD results were confirmed through SEM images. Particle sizes comply with the XRD results. It was observed from the surface images of films that surface appearances of ZnS (0.10 M) and ZnS (0.15 M) films were similar to each other and spherical particles were randomly positioned on the surface. From the SEM images, it was observed that both films well adhered to the glass substrates.

3.2 FTIR and Raman spectroscopy

In this study, FTIR and RAMAN studies were done to confirm ZnS formation and determine other functional groups on the surface of films. Absorption spectra in the middle infrared zone cover approximately 600-5000 cm^{-1} wave numbers. The spectrum gap between 3600-1200 cm^{-1} is called functional groups zone. The second one is the 500-1200 cm^{-1} gap called as the fingerprint zone. This zone is especially used for analyzing small structural and composition changes of molecules. Vibration frequency of a link is extremely influenced by a group next to one of its atoms or other atoms. Therefore, a group frequency is not given by a value, it is given by a gap [22]. FITR spectra of ZnS films produced in this study are given in Fig. 3. When, FTIR spectra of the films were analyzed, it was observed that there was not any significant difference with respect to their functional groups. The spectral bands between 500 and 700 cm^{-1} are related with characteristic Zn-S stretching and revealed its presence in the layers. These results comply with the literature [7, 23,24]. The peaks of all films observed in this gap are symmetrical and their intensities are almost the same. The intensive peak observed at 900-1000 cm^{-1} gap belongs to C-O vibration mode [25,26]. The spectral bands at 2063 cm^{-1} and 2400 cm^{-1} were related with C-H stretching vibrations [27]. Just like infrared spectroscopy, Raman spectroscopy is established on vibration energy. Raman shifts are not based on the wave number of excitant beam, but on the studied material. The Raman spectra of ZnS films are seen in Fig. 3b. The peak around 450 cm^{-1} observed on ZnS(0.10 M) with ZnS(0.15 M) high crystallization degrees can be attributed to S\\S vibration mode [28-30]. It was concluded that the peaks observed at 600 cm^{-1} and 800 cm^{-1} in spectra of ZnS(0.10M) and ZnS(0.15M) films belong to ZnS vibration mode in accordance with compliance with FTIR spectra. The peak observed at 900-1000 cm^{-1} gap belongs to C-O vibration mode.

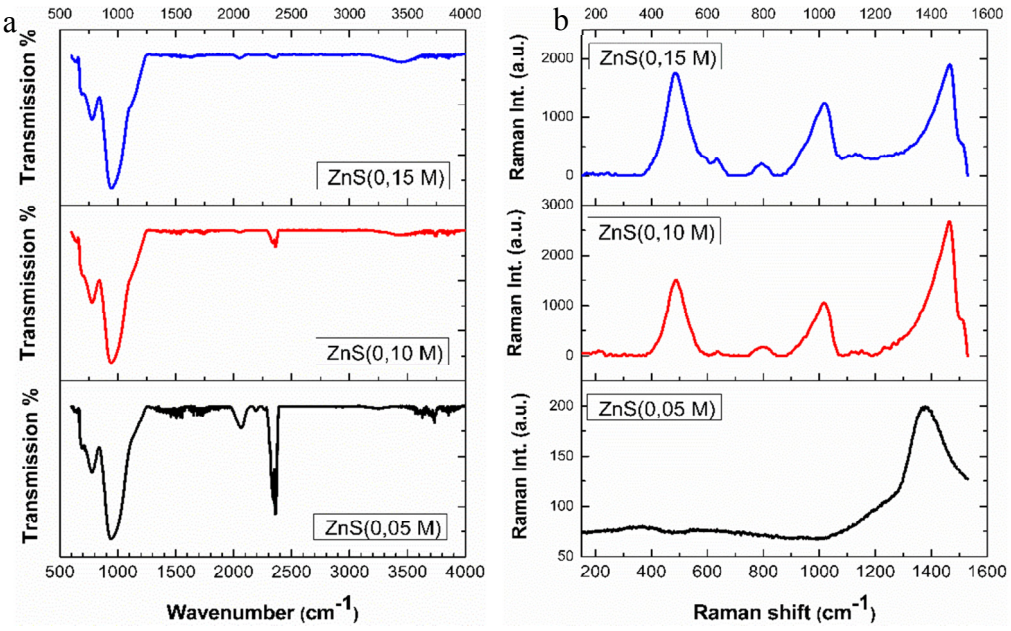

Fig. 3. (a) FTIR spectra and (b) Raman spectra of the ZnS nanostructured films.

When, the energy of Raman shifts of the links in a molecule are equal to the energy of infrared absorptions of the same molecule, the Raman and infrared peaks coincide [22]. These peaks did not arise clearly at 200-1000 cm^{-1} gap of ZnS(0.05 M) film. This film with low crystallization degree is the film which was prepared with the aqueous solution in the lowest concentration. Probably, the ZnS vibration modes could not be determined for this film due to the deficiency of ZnS crystals. It is considered that the Raman peaks at 1400 cm^{-1} observed on all films come from the substrate glass as they are very thin.

3.3 *UV-visible studies*

Determining the optic coefficients of II-VI group semiconductors which are frequently used in optoelectronics field is one of the most important steps for producing materials suitable for the purpose. Optic absorption, reflectance and transmittance spectra are used as tools for determining the absorption limit, allowed or forbidden, direct or indirect optic transitions, forbidden energy band gap and optical coefficients.

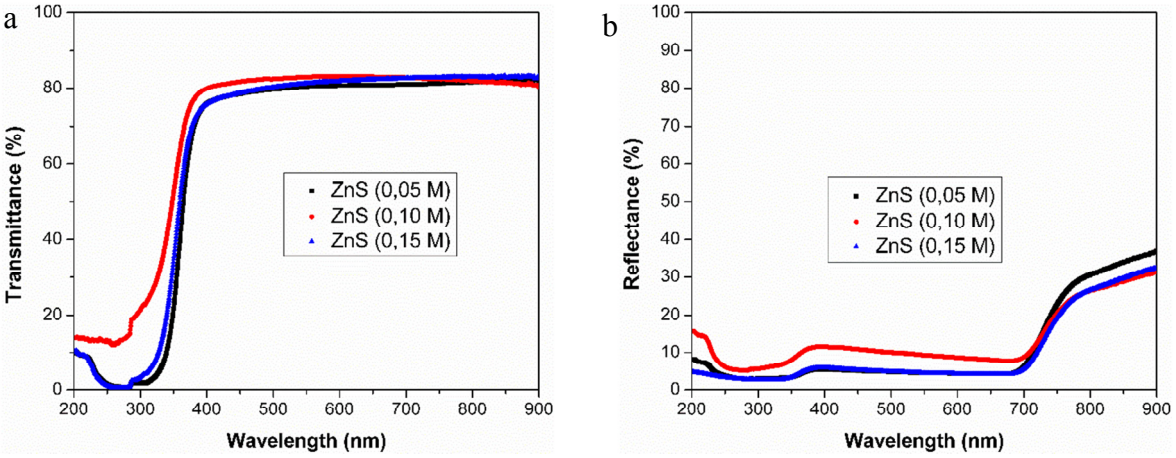

Fig. 4. (a) The transmittance spectra and (b) the reflectance spectra of ZnS nanostructured films.

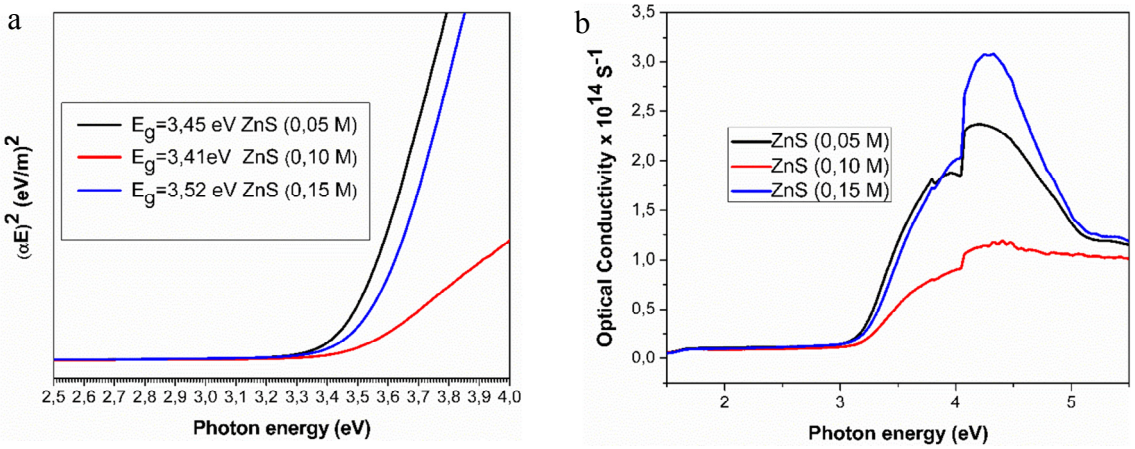

Fig. 5.(a) The plot of $(\alpha hv)^2$ vs. photon energy of the films and (b) variation of optical conductivity of the films with photon energy.

In this study, optical transmittance and reflectance spectra of the films were taken and shown in Fig. 4a and 4b. As molarity increased, transmittance edge shifted towards smaller wavelengths. The highest transmittance value at 350 nm value belongs to ZnS (0.10M) film with 85%. Transmittance and reflectance spectra of ZnS(0,05 M) and ZnS(0.15 M) films showed a variation similar to their wavelength. Forbidden energy gaps of ZnS (0.05 M), ZnS (0.10 M) and ZnS (0.15 M) films were found respectively as 3.45 eV, 3.41 eV and 3.52 eV and shown in Fig. 5a. The forbidden energy gap values determined for the ZnS films are lower than 3.77 eV [2] value estimated for bulk hexagonal wurtzite ZnS [21]. This decline in the forbidden energy gap value can be attributed to defects and local bond distortion as well as intrinsic surface states and interfaces which yield localized electronic levels within the forbidden energy gap, due to electron transitions from the valence band to the conduction band [21]. The extinction coefficient (k) and refractive index (n) values of the films are also seen in Fig. 6a and 6b. The extinction coefficient and refractive index values of the films varied depending on the wavelength of the incoming light. The extinction coefficient values of the films decreased range of 350-900 nm. The optical conductivity values seen in Fig. 5b began increasing around 3 eV for all films and reached their maximum values around 4.25 eV.

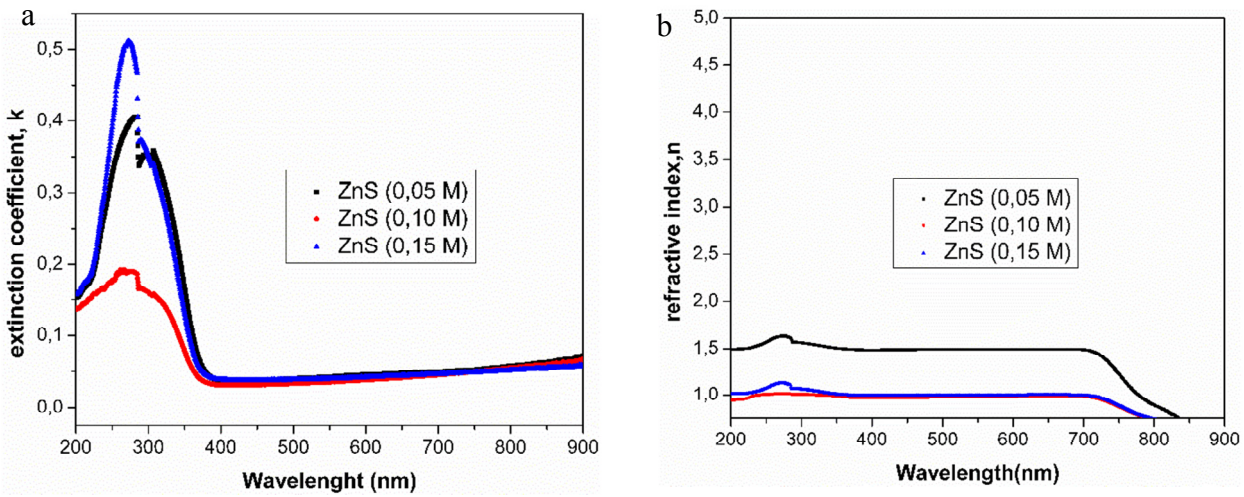

Fig. 6. (a) Variation of extinction coefficient and (b) variation of refractive index of the films with wavelength.

4. Conclusion

ZnS films were produced by spraying aqueous solutions prepared in different molarities and mixed in same amounts on glass bases heated up to 300±5°C. 150 ml solution was sprayed in total. The effects of various molarities on structural and optical properties of ZnS films were analyzed. It was determined by XRD analyses that the molarity change has its strongest impact on crystallization level. It was determined by XRD and SEM images that the crystallization sizes of films were at nm scale. Optical properties of the films were analyzed through optic transmittance and reflectance spectrums. The extinction coefficient and refractive index values of the films were calculated by means of their absorbance and transmittance spectra. When, optical conductivity values of films were compared, it was observed that the film produced at the highest molarity has the highest optical conductivity value.

Acknowledgements

Hereby, we thank Mrs. Vildan Bilgin for help with the production of the films, Mrs. Özge Baglayan for the Raman spectroscopy, Mrs. Seval Aksoy for UV-vis measurements.

References

[1] S.R. Chalana, R. Jolly Bose, R. Reshmi Krishnan, V.S. Kavitha, R.Sreeja Sreedharan, V.P. Mahadevan Pillai, J.of Phys. and Chem. of Solids 95 (2016) 24–36.
[2] X. Fang, T. Zhai, U.K. Gautam, L. Li, L. Wu, Y. Bando, D. Golberg, Mater. Sci. 56 (2011) 175–287.
[3] L. Xuanjie, X. Cai, J. Mao, C. Jin, Appl. Surf. Sci. 183 (2001) 103–110.
[4] M.C. Schlamp, X. Peng, A.P. Alivisatos, J. Appl. Phys. 82 (1997) 5837–5842.
[5] S. Biswas, M.F. Hossain, T. Takahashi, Thin Solid Films 517 (2008) 1284–1288.
[6] R. W. Miles, G. Zoppi, K. T. Ramakrishna Reddy, I. Forbes, Organic Nanostructured Thin Film Devices and Coatings for Clean Energy, CRC Press, London, 2010.
[7] K. Nagamani, P. Prathap, Y. Lingappa, R. W. Miles, K.T. R. Reddy, Physics Procedia 25 (2012) 137–142.
[8] L.X. Shao, K.H. Chang, H.L. Hwang, Appl. Surf. Sci. 212 (2003) 305–310.
[9] W. Witte, S. Spiering, D. Hariskos, Dunne Schicht 26 (2014) 23–27.
[10] W. Daranfed, M.S. Aida, A. Hafdallah, H. Lekiket, Thin Solid Films 518 (2009) 1082–1084.
[11] S.P. Patel, S.A. Khan, A.K. Chawla, R. Chandra, J.C. Pivin, D. Kanjilal, L. Kumar, Physica B 406 (2011) 4150–4154.
[12] M. Ashraf, S. Ullah, S. Hussain, A.H. Dogar, A. Qayyum, Applied Surface Science 258 (2011) 176– 181.
[13] W. Li, J. Chen, S. Cheng, Y. Wang, J. Semicond. 35 (2014) 023001-023005.
[14] P. Vasekar, T. Dhakal, L. Ganta, D. Vanhart, S. Desu, Thin Solid Films 524 (2012) 86–92.
[15] N. Bouguila, D. Bchiri, M. Kraini, A. Timoumi, I. Halidou, K. Khirouni, S. Alaya, J. Mater. Sci. Mater. Electron. 26 (2015) 9845–9852.
[16] P.A. Luque, A. Castro-Beltran, A.R. Vilchis-Nestor, M.A. Quevedo-Lopez, A. Olivas, Mater. Lett. 140 (2015) 148–150.
[17] A. Jrad , T. B. Nasr, N. Turki-Kamoun, Optical Materials 50 (2015) 128–133.
[18] N. Bitri, K. Ben Bacha, I. Ly, H. Bouzouita, M. Abaab, J Mater Sci: Mater Electron 28 (2017) 734–744.
[19] P.O. Offor, A.C. Nwanya, A.D. Omah, C.C.D. Mkpume, M. Maaza, B.A. Okorie, F.I. Ezema, J Solid State Electrochem 21 (2017) 2687–2697.
[20] R. Mendil, Z. Ben Ayadi, K. Djessas, J.of Alloys and Compounds 678 (2016) 87-92.
[21] F. A. La Porta, J. Andres, M. S. Li, J. R. Sambrano, J. A. Varela, E. Longo, Phys. Chem. Chem. Phys. 16 (2014) 20127-20137.
[22] T.Gündüz, İnstrümental Analiz ninth ed. Gazi, Ankara, 2005.
[23] D.A. Reddy, S. Sambasivam, G. Murali, B. Poornaprakash , R.P. Vijayalakshmi, Y. Aparna, B.K. Reddy, J.L. Rao, J. of Alloys and Compounds 537 (2012) 208–215.
[24] N. Shanmugam, S. Cholan, N. Kannadasan, K. Sathishkumar, G. Viruthagiri, Spectrochimica Acta Part A: Molecular and Biomolecular Spectroscopy 118 (2014) 557–563.
[25] D. A. Reddy, G. Murali, R.P. Vijayalakshmi, B.K. Reddy, Appl Phys A 105 (2011) 119–124.
[26] L.S. Devi, K.N. Devi, B.I. Sharma, H.N. Sarma, J. of App. Phys. 6, (2014) 06-14.
[27] M. Sudha, S Senthilkumar, R. Hariharan, A. Suganthi, M. Rajarajan, J. Sol-Gel Sci. Technol. 65 (2013) 301–310.
[28] N. Prasad, K. Balasubramanian, Spectrochimica Acta Part A: Molecular and Biomolecular Spectroscopy 173 (2017) 687–694.
[29] Z. Abdullaeva, E. Omurzak, T. Mashimo, Int. J. Chem. Mol. Nucl. Mater. Metall. Eng. 7 (6) (2013) 422–425.
[30] J. Rodríguez-Moreno, E. Navarrete-Astorga, E.A. Dalchiele, R. Schrebler, J.R. Ramos-Barrado, F. Martín, Chem. Commun. 50 (2014) 5652–5655.